© Federation of European Neuroscience Societies

Computer model of passive signal integration based on whole-cell *in vitro* studies of rat lateral geniculate nucleus

Adam M. Briska,[1] Daniel J. Uhlrich[1] and William W. Lytton[1,2]

[1]Department of Anatomy, Neuroscience Training Program, University of Wisconsin
[2]Departments of Physiology, Pharmacology and Neurology, State University of New York, Downstate, 450 Clarkson Ave., Box 31, Brooklyn, NY 11203, USA

Abstract

Computer models were used to investigate passive properties of lateral geniculate nucleus thalamocortical cells and thalamic interneurons based on *in vitro* whole-cell study. Two neurons of each type were characterized physiologically and morphologically. Thalamocortical cells transmitted 37% of steady-state signal orthodromically (distal dendrite to soma) and 93% antidromically (soma to distal dendrite); interneurons transmitted 18% orthodromically and 53% antidromically. Lowering membrane resistance caused a dramatic drop in steady-state signal transmission. Simulation of brief signals such as orthodromically transmitted postsynaptic potentials and antidromically transmitted action potentials showed relatively poor transmission due to the low-pass filtering property of dendrites. This attenuation was particularly pronounced in interneurons. By contrast, bursts of postsynaptic potentials or action potentials were relatively well transmitted as the temporal summation of these recurring signals gave prolonged depolarizations comparable to prolonged current injection. While synaptic clustering, active channels and reduction of membrane resistance by ongoing synaptic activity will have additional profound effects *in vivo*, the present *in vitro* modelling suggests that passive signal transmission in neurons will depend on type of signal conveyed, on directionality and on membrane state. This will be particularly important for thalamic interneurons, whose presynaptic dendrites may either work independently or function in concert with each other and with the soma. Our findings suggest that bursts may be particularly well transmitted along dendrites, allowing firing format to alter the functional anatomy of the cell.

Introduction

The two main cell types in thalamic nuclei, thalamocortical cells and thalamic interneurons, play different roles in the thalamic circuit. They possess very different dendritic tree morphologies, which can be expected to strongly influence their respective signal transmission properties. Thalamocortical cells, which project an axon to cortex, have somewhat shorter dendrites. In contrast, the inhibitory interneurons have long, thin dendrites that branch repeatedly to form elaborate arbors. Dendritic signal integration and transmission in the thalamocortical cells will determine the passage of many afferent inputs, including sensory information, to cortex (Wilson *et al.*, 1984; Sherman & Guillery, 1996). Interneuron dendrites also receive synaptic contacts from many parts of the brain and form synapses with other interneurons and with thalamocortical cells (Jones, 1985; Pasik *et al.*, 1976; Hamos *et al.*, 1985). Dendritic signalling properties will have particular significance in interneurons because their dendrites are both pre- and postsynaptic. Greater signal spread in interneuron dendrites would permit coordinated transmission via the axon and via multiple dendrodendritic synapses, potentially influencing many postsynaptic cells.

An early modelling study by Bloomfield & Sherman (1989) found thalamocortical cells to be electrotonically compact and interneurons to be electrotonically large. This meant that, while a synaptic signal generated anywhere in a thalamocortical cell dendrite would be transmitted throughout the arbor and to the soma, it was concluded that distal dendrites of interneurons were functionally isolated from the soma and other dendrites, suggesting that each interneuron might consist of many independent dendritic domains. The thalamocortical cell aspect of this study has been superseded by the findings of Neubig & Destexhe (2001).

Although these authors were able to replicate the prior findings of Bloomfield & Sherman (1989), they noted that this depended on simplifications which, in retrospect, were not warranted. Using improved methodology with a full 1416-compartment model, this more recent study found that, although synapses at all dendritic locations communicated >79% of their charge to the soma, >80% of the dendritic tree had relatively little effect on somatic voltage due to dispersal of charge back out other dendrites. While noting thalamocortical cells to be electronically compact (defined by tip-to-soma paths of $\approx 0.35\,\lambda$, where λ is the length constant), they noted that this steady-state measure was of limited use in assessing response to temporally brief synaptic response. Using synaptic signals, they found thalamocortical cell dendrites would group into functionally distinct 'clusters' with focal activity which differed from the bulk response of the rest of the cell. These Neubig & Destexhe (2001) thalamocortical cell 'clusters' are comparable to the Bloomfield & Sherman (1989) interneuron dendritic 'domains'. Therefore it has been suggested that regions of dendritic tree could do independent information processing in both cell types.

Neubig & Destexhe (2001) reassessed the modelling of thalamo-cortical cells. However, the electrotonic properties of interneurons have not been re-addressed using more recent modelling techniques. In addition to improvements in modelling, the physiological data have changed as studies using whole-cell recording have yielded higher values for input resistance (R_{in}) than older studies which used sharp impalement (Storm, 1990; Staley *et al.*, 1992). In particular, we found substantially higher values in interneurons (Zhu *et al.*, 1999a). Higher R_{in} values grossly translate to higher membrane resistance and shorter length constants and would be expected to change cell responses *in vitro*. Membrane resistance *in vivo*, on the other hand, will vary greatly depending on varying conductances due to ongoing synaptic activity.

Portions of these data have previously appeared in abstract form (Briska *et al.*, 1999).

Materials and methods

We used our previously published data from interneuron and thala-mocortical cell whole-cell patch recordings (Zhu *et al.*, 1999a,b,c). Physiological measurements were made at 34 °C and utilized small hyperpolarizing current to minimize the effects of active channels. For modelling, we chose two thalamocortical cells and two interneurons where the full 3-dimensional dendritic tree was recovered without edge-of-slice truncation. Cells were identified anatomically and reconstructed using the Neurolucida system (Fig. 1). We corrected for shrinkage based upon the overall tissue shrinkage. The tissue shrank by ≈10% horizontally and ≈50% vertically. Anatomical and physiological values for these four cells are given in Table 1. Dendritic diameter values are not given because these are not always reliable, with distal dendrite diameters in interneurons being typically below light resolution. The usual limit for light resolution (≈0.5 μm) is even worse when using intracellular labelling within slices of >5 μm thick (ours were 60 μm). In our material, this was primarily a problem with shafts that interconnect the presynaptic dendritic specialisations of interneurons. We therefore estimated these values based on prior electron microscopy (Hamos *et al.*, 1985).

Adult Sprague–Dawley rats (100–300 g) were deeply anesthetized with halothane. Following decapitation, the brain was removed quickly, sectioned at 500 μm and placed in oxygenated physiological solution. Selected slices containing the lateral geniculate nucleus were chosen for whole cell electrophysiological study. Additional details are provided by Zhu *et al.* (1999c). Experiments were carried out in accordance with NIH and University of Wisconsin guidelines (UW Animal Use Review Committee) regarding the care and use of animals for experimental procedures.

Passive parameters were obtained by fitting physiological recordings of the cells' responses to single, low-amplitude hyperpolarizing current pulses using the principal axis method implemented in NEURON software (Hines, 1993, 1994). Although some of the cells showed evidence of anomalous rectification, this was small enough to not substantially effect the approximations. We have presented modelling of the interneuron anomalous rectifier in a previous paper (Zhu *et al.*, 1999a).

Transient signal transmission simulations were run using voltage clamp of waveforms comparable in shape to postsynaptic potentials (PSPs) and action potentials (APs). The PSP analogue was a half sine wave with amplitude of 10 mV and duration of 5 ms. The AP analogue was a half sine wave of amplitude 70 mV and duration 2 ms. Because these signals were voltage, rather than current or conductance, change, each signal permitted the entry of a limited amount of current. In the case of the AP analogue, this is comparable to the rapid activation and termination mediated by sodium influx and potassium efflux, respec-

tively. In the case of PSP analogue, this would correspond to an excitatory PSP (EPSP) that was quickly terminated by the arrival of a shunting or hyperpolarizing inhibitory PSP (IPSP), whether feedback or feedforward. Such coactivation is also likely to be present in the case of the synaptic triad which involves colocalization of an afferent synapsing onto both an interneuron and a thalamocortical cell with a complex that also includes an interneuron-to-thalamocortical cell dendrodendritic synapse. Use of voltage-clamp PSP allowed us to assess temporal summation associated with dendritic conduction independent of local summation at the synaptic location. Both signals were implemented in NEURON using the Vector Class to produce (apply) a half cycle of a sine wave. This was then read into a voltage clamp (VClamp) using the Vector play command.

As a primary measure, we calculated a scaled electrotonic distance (D_{xfer}) using transfer impedances. This was calculated as the distance from soma to distal injection or measurement point divided by the log of voltage ratios at the two points. D_{xfer} gives a generalized analogue of length constant that can be readily determined for any pair of stimulating and recording sites. In an infinite cable, the scaling would give $D_{xfer} = \lambda$ at all measurement locations.

At a given distance from the soma, we found varying degrees of scatter for signal amplitude, correlating with different dendritic diameters or with different termination distances. To summarize the data, we averaged across results for locations at a given distance. For orthodromic signals, soma signals arising from different dendrites at a given distance were averaged. For antidromic signals, signals in different dendrites at a given distance arising from signals placed in the soma were averaged.

We chose different signal amplitudes for antidromic and orthodromic study to be consistent with the approximate size of an action potential or postsynaptic potential, respectively. Although amplitude is not relevant when studying these linear properties, it will be important when active properties are studied in the future. Similarly, we express results both in mV transmission and percentage transmission so that absolute as well as relative effects can be appreciated. Transmission measurements are based on peak voltages.

Our study was primarily designed to compare the transmission of transient signals to those of steady state signals. To this end, we chose compromise waveforms that were intermediate in duration and frequency relative to the expected inputs that would be seen in thalamocortical cells and interneurons, both of which receive different frequency inputs from periphery, reticularis cells and neocortex. These frequency differences pertain both to the intrinsic frequencies of the single signal and to the burst frequency. We chose a burst frequency of 200 Hz. This relatively high burst frequency is in the physiological range for a variety of cell inputs of interest, including interneurons, thalamocortical cells and retinal afferents arriving in thalamus (Mastronarde, 1987; Zhu *et al.*, 1999b). We also varied burst frequency.

As an alternative approach, we could have employed a white-noise analysis, representing all frequencies. A white-noise study would more completely characterize passive electrical properties, but would not be as readily interpretable in a neurobiological context. However, we agree with Neubig & Destexhe (2001) that a study of biologically relevant signals is more readily interpreted and more readily extended to the active-dendrite case.

Alternatively, a more detailed approach would involve customising the inputs tested according to the characteristics of presynaptic cell firing, location on the dendrites and type of synapse. However, because we wished to do comparison between cell types, we opted to study a uniform set of signals to allow for direct comparison. Additionally, because this is a passive study, there is no concern with frequency-
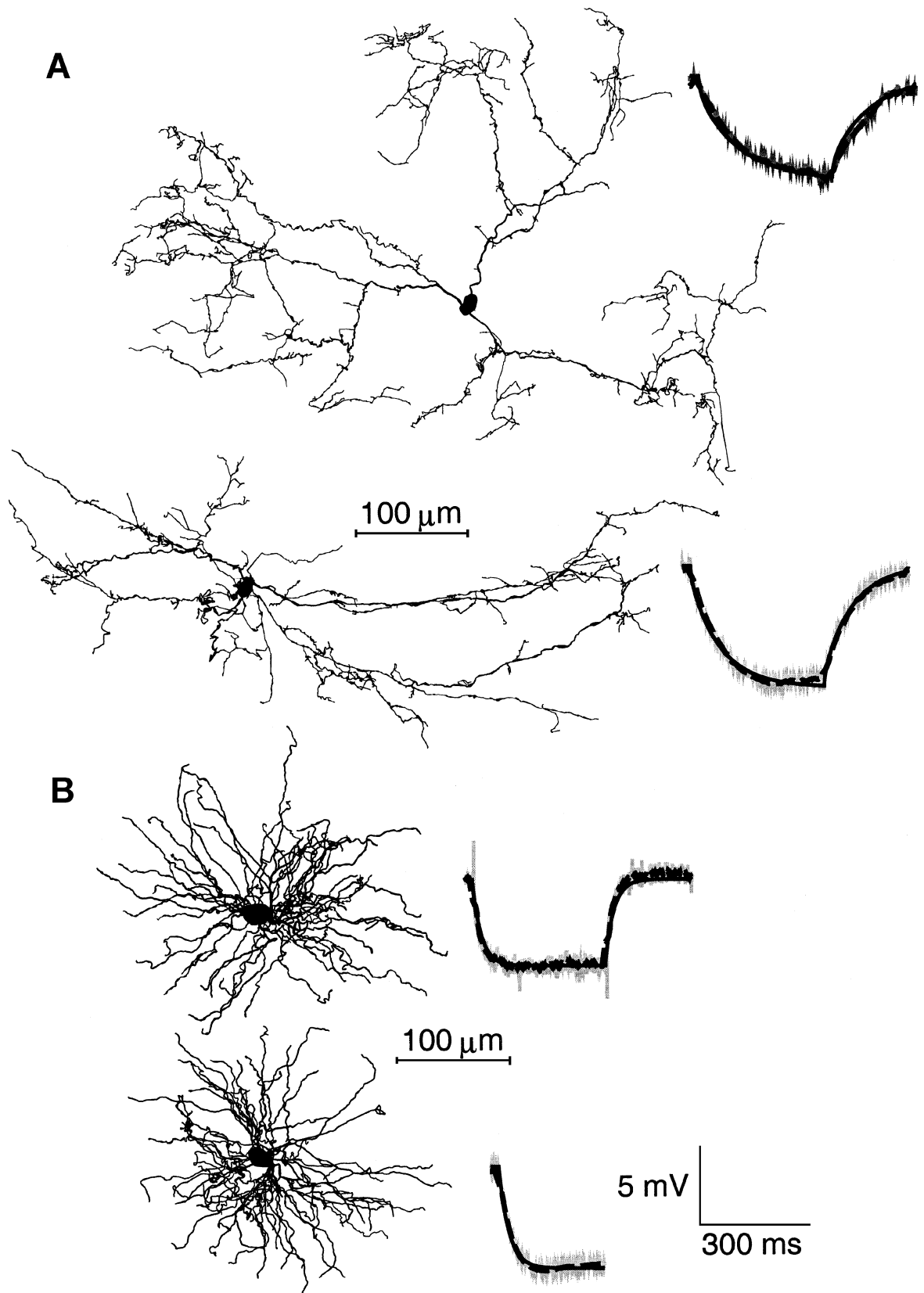
FIG. 1. Cells used in simulation: anatomy and fitting curves for the cells used in the simulations. The traces represent recordings of somatic voltage with constant hyperpolarizing current injection in the soma (grey line, physiology; dashed line, smoothed; black line, model). Two cells of each type are shown with the corresponding physiology. (A) Thalamic interneurons of rat lateral geniculate nucleus. Current, $-12.5\,\mathrm{pA}$. (B) Thalamocortical relay cells of rat lateral geniculate nucleus. Current, $-50\,\mathrm{pA}$.

TABLE 1. Membrane properties: physiological values for each cell modelled

Cell	R_{in} (MΩ)	τ_m (ms)	Area (μm^2)	Length (μm)	Max.Length (μm)
TC$_A$	103	25	22897	154 ± 46	(244)
TC$_B$	126	26	24675	156 ± 46	(233)
TI$_A$	512	76	23359	445 ± 158	(724)
TI$_B$	589	82	19231	357 ± 166	(775)

TC, thalamocortical cells; TI, thalamic interneurons.

dependent resonances. This will have to be addressed in subsequent active-dendrite research.

Simulations were run in NEURON (Hines, 1993, 1994) using 150- and 196-compartment thalamocortical cell models and 657- and 398- compartment interneuron models on a Sun Ultrasparc 2 workstation (Sun Microsystems Inc., Santa Clara, CA, USA). We did not use a formal method for spatial segmentation but instead evaluated our results with a larger number of compartments to verify the adequacy of spatial approximation. In addition to using our hand-tailored signals, we also used the Impedance tool of NEURON to check the results using sinusoidal signals of comparable frequency.

Results

Defining cell parameters

Over 3000 simulations were run to determine membrane parameters and to explore signal responses. Membrane parameters were fitted to physiological traces using the principal axis fitter in the NEURON simulator. The three parameters fitted were membrane resistance (R_m), membrane capacitance (C_m) and axial resistance (R_a). For each individual cell we chose a low-amplitude hyperpolarized trace that was not overly contaminated with synaptic potentials, active anom- alous rectification, or noise. The model charging curves closely matched physiology (Fig. 1). The parameters used for further study were averaged from the two cells of each cell type (Table 2). In addition to utilizing parameters based on our measurements (high- R_m case), we also used a set of parameters with a five-fold reduction in R_m (low-R_m case). These parameters were chosen to be comparable both to previous *in vitro* studies done with sharp electrodes and to the *in vivo* situation of reduced R_m due to synaptic bombardment (Bernander *et al.*, 1991; Neubig, 1999).

Because our physiological measurements were made from the cell soma, we only indirectly measured properties of the dendritic tree. Consequently, we were concerned that parameters whose influence is greatest in the dendrites might not be constrained with somatic measurements. In particular, axial resistance reflects the falloff of current as it passes through the dendrites and has been shown to be poorly constrained by somatic measurements (Kapur *et al.*, 1997a,b; Chitwood *et al.*, 1999). As expected, the influence of R_a was critical for the transmission of signal along the dendrite for both interneurons (Fig. 2A) and for thalamocortical cells (not shown). A low R_a of

TABLE 2. Parameters used in simulations

Cell	E_{rest} (mV)	R_a (Ωcm)	C_m ($\mu F/cm^2$)	R_m (kΩcm^2)	Low R_m (kΩcm^2)
TC	−62.7	100	0.85	30.3	6.1
TI	−54.5	70	1.00	95.2	19.0

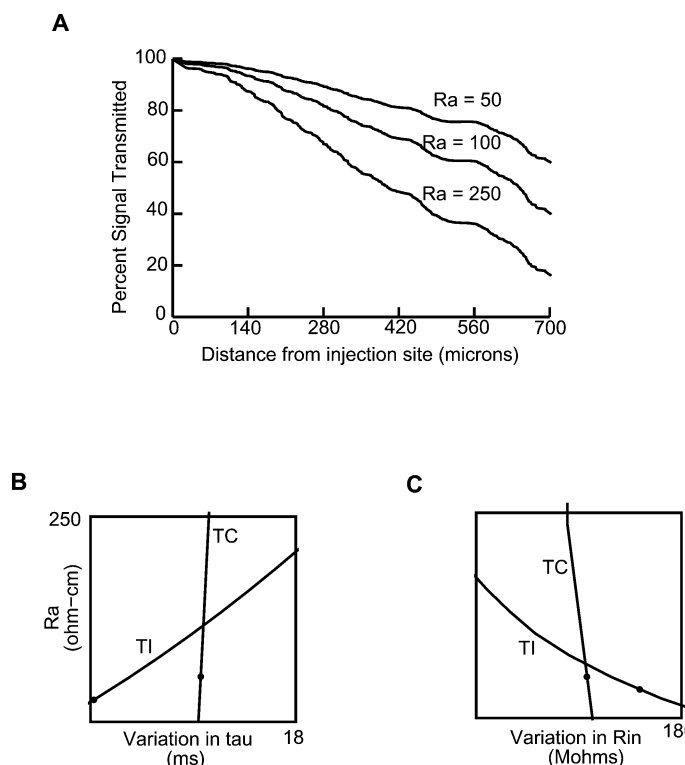TC, thalamocortical cells; TI, thalamic interneurons.

FIG. 2. Parameter sensitivity for axial resistance (R_a). (A) Steady-state signal transmitted from the interneuron distal dendrites with varying R_a values (50– 250 Ωcm). Increase in R_a substantially reduced signal transmission. (B) Best-fit parameter sensitivity of R_a to variation in τ_m. τ_m does not constrain R_a in thalamocortical cell model but does in interneuron model (thin curve). Curves are on same scale for y-axis but τ_m values are relative and centred. Best-fit simulation parameters are indicated by filled circles. (C) Best-fit parameter sensitivity of R_a to variation in R_{in}. Graph organization as in B. Once again the interneuron is fairly well constrained but the thalamocortical cell is not.

50 Ωcm, comparable to that found in squid axons, allowed ≈60% signal transmission from soma to the distal dendrites in the interneur- ons. By contrast, use of the high R_a (250 Ωcm) reported in some mammalian studies permitted only ≈15% transmission.

In order to quantify the accuracy of our parameter identification, we performed a parameter-sensitivity analysis. In the fitting process, all model parameters were varied by the algorithm in order to match measured values. This implicitly provided a detailed fit to the multiple exponentials of the charging curve. In parameter-sensitivity analysis, we varied a single parameter and recorded the effects on the physio- logically measurable values of apparent R_{in} and membrane time constant (τ_m). These apparent values are obtained by evaluating the charging curve as if it were a single exponential. Then, we swapped the axes in order to show how changes in the measurable values would alter the value of the parameter determined by the fitting process. As expected, the R_m and C_m parameters were very sensitive to variation of R_{in} and τ_m around the measured values. R_m varied strongly with R_{in}, and C_m varied with changes in both R_{in} and τ_m (not shown). On the other hand, R_a in the thalamocortical cell showed extremely little parameter sensitivity (Fig. 2B and C), a lack of effect comparable to what we previously found in pyramidal cells (Kapur *et al.*, 1997b; Appendix C of Kapur *et al.*, 1997b). The fitting algorithm suggested an R_a of 100 Ωcm for the thalamocortical cell, consistent with values used in other studies. However, the lack of a strong dependence of R_a on measured values provided little confidence in this value, as values between 50 and 200 Ωcm could have adequately fitted the curves.

By contrast, our interneuron model showed good R_a parameter sensitivity (Fig. 2B and C). Unlike the thalamocortical cells, whose broad, short dendrites provided relatively easy access to large areas of dendritic membrane, the long, thin dendrites of the interneurons restricted the amount of membrane accessible from soma and amplified the importance of R_a. Low R_{in} in the interneuron model was fitted with a low R_a, which increased access to the distal dendrites, providing a greater surface area for loss of current injected into the soma. Similarly, low R_a was also associated with a longer time constant in the interneuron model, because of the time required for current passage and charging of the large dendritic tree. Our R_a value of $70\,\Omega$cm for the interneuron places it in a range where relatively small

changes in R_{in} or τ_m measurements would be expected to substantially change its estimation. This value, while differing from some previous estimates based on modelling in other cell types (Major *et al.*, 1993a, b; Chitwood *et al.*, 1999) is comparable to values obtained directly using dual electrodes in soma and dendrite of neocortical pyramidal neurons (Stuart & Spruston, 1998).

Steady state

Initially we assessed the transmission of constant (steady-state) voltage signals. In addition to the orthodromic (dendrite to soma) signals, we also examined antidromic (soma to dendrite) signal propagation, comparable to voltage-clamp experiments. We performed the
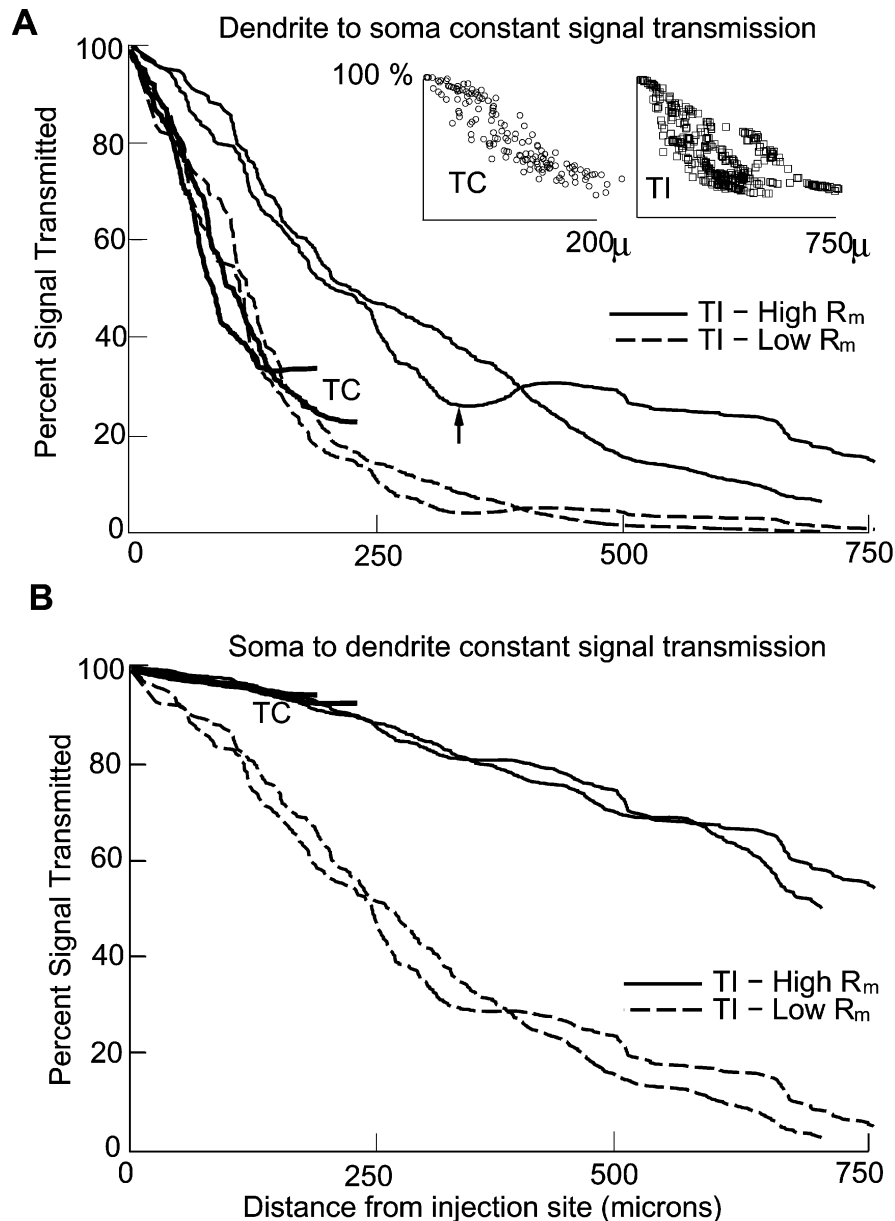

FIG. 3. Steady state signal attenuation: thick lines, thalamocortical cells; thin lines, interneurons. For this and subsequent figures, each trace shows the average for all dendritic compartments found at the given distance from the soma. Parameters as given in Table 2. (A) Orthodromic transmission. Constant current (0.1 nA) was injected into locations throughout the dendritic tree with measurement of voltage in the soma. Voltage at the soma were divided by the corresponding voltage (at the injection site). All values from a given distance were then averaged. Arrow shows a dip in the curve at a location where several thin dendrites terminated. Abscissa values are distances from injection site to soma. Insets: full data set for one thalamocortical cell and one interneuron. (B) Antidromic transmission. Constant current (0.1 nA) was injected into the cell soma. Voltages measured at all points in the dendritic tree are divided by this soma voltage. All values at a given distance are averaged to generate the curves in the main figure.

simulations on both of our thalamocortical model cells and both interneuron model cells (Fig. 3). The traces show the drop-off at a given distance toward (Fig. 3A) or away from (Fig. 3B) the soma. Values are averages taken from all dendritic compartments at the given distance from the soma. Interneuron and thalamocortical cell traces are readily distinguished: the interneuron dendrites are much longer so the traces extend the length of the graph (750 µm) while the thalamocortical cell traces terminate at ≈250 µm. Rather than showing error bars, which would obscure the graph, we give the raw data for one example of each cell type in the insets to indicate the spread of values.

In Fig. 3, both models of each cell are shown. Both cells of a type showed similar results, demonstrating that global dendritic effects were comparable despite differences in detail. To simplify subsequent figures, we only show results for one model of each type because similar results were obtained with the second cell.

Voltage clamping a single compartment in the distal dendrite of the thalamocortical cells with signal measurement in the soma (Fig. 3A) indicated relatively mild signal loss, with transmission of ≈37% ($D_{xfer} = 228$ µm). As previously found by Neubig & Destexhe (2001), fall-off was considerably greater than that found by Bloomfield & Sherman (1989) despite the fact that we were using a far higher membrane resistance: $30.3 \, \text{k}\Omega\text{cm}^{-2}$ compared to $5.5 \, \text{k}\Omega\text{cm}^{-2}$ in Bloomfield & Sherman (1989). This difference was probably due to differences in the geometry of the models. Bloomfield & Sherman (1989) used a single traced dendrite which gave idiosyncratic results not consistent with the behaviour of the neuron as a whole (Neubig & Destexhe, 2001).

Orthodromic steady-state signal transmission from interneuron distal dendrites showed signal transmission of 18% ($D_{xfer} = 444$ µm), more signal transmission than reported by Bloomfield & Sherman (1989). The greater transmission can be explained by the higher R_m in this study. The dip in the transmission curve for one of the traces (upward arrow) is due to a number of thin terminal dendritic branches at this distance from the soma. The poor voltage transmission through these thin dendrites reduced the average at this distance.

Antidromically, simulated voltage clamp in the soma showed greater transmission to the distal dendrites than was seen in the opposite direction (Fig. 3B). This was expected because the orthodromically transmitted signal flows from the narrow dendrites into the low-impedance current sink provided by the soma, the broad proximal dendrites and the rest of the dendritic tree, while antidromic signals flow from the large soma to the narrow, high input impedance dendrites (Wathey *et al.*, 1992). The thalamocortical cells showed an average antidromic transmission of 93% ($D_{xfer} = 3322$ µm) and the interneuron dendrites showed total average transmission of 53% ($D_{xfer} = 1150$ µm).

We also assessed the effects of reducing input resistance five-fold, providing a far leakier membrane more comparable to that obtained from sharp electrode impalement studies or the reduced membrane resistance caused by synaptic bombardment *in vivo*. As expected, this membrane resistance produced far less signal transmission both orthodromically and antidromically, as more current was able to escape along the membrane. Looking first at the orthodromic measure, the thalamocortical cells showed a transmission of 4% (not shown; $D_{xfer} = 99$ µm) and the interneurons 2% transmission (Fig. 3A, dashed lines; $D_{xfer} = 193$ µm). These values for the interneurons matched the results of Bloomfield & Sherman (1989). Antidromically, the decrease in transmission was also pronounced. The thalamocortical cells showed a transmission of 70% (not shown; $D_{xfer} = 672$ µm). The interneurons showed a larger change, dropping to 5% transmission (Fig. 3B, dashed lines; $D_{xfer} = 252$ µm).

Brief signal

The steady-state measures reflect the way responses are typically assessed experimentally. However, continuous membrane current is not seen biologically, where signals are transient. Therefore, we looked at transmission of signals using orthodromic waveforms similar to compound postsynaptic potentials (EPSP–IPSP sequence, hereafter EPSP–IPSP) and antidromic waveforms similar to action potentials. Overall, transmission of these brief signals was considerably less than seen with the steady-state signals. Orthodromically, the thalamocortical cells transmitted 8% (0.8 mV) and the interneurons transmitted only 1% (0.1 mV) of the EPSP–IPSP analogue from two-thirds out on the dendrite (Fig. 4A). Antidromically, the AP analogue produced a 50% (35 mV) signal two-thirds out on the dendrite for the thalamocortical cells, but only 1.4% (1 mV) transmission in the interneurons (Fig. 4B).

Basic cable theory predicts poor transmission of high-frequency signals compared to steady-state or low-frequency signals. This is due to the cable serving as a low-pass filter, with high-frequency components shunting to ground through the capacitive limb of the parallel conductance model for each compartment. We confirmed this in our morphologically complex model by varying membrane capacitance alone without changing R_m in the interneuron model. Such a change in
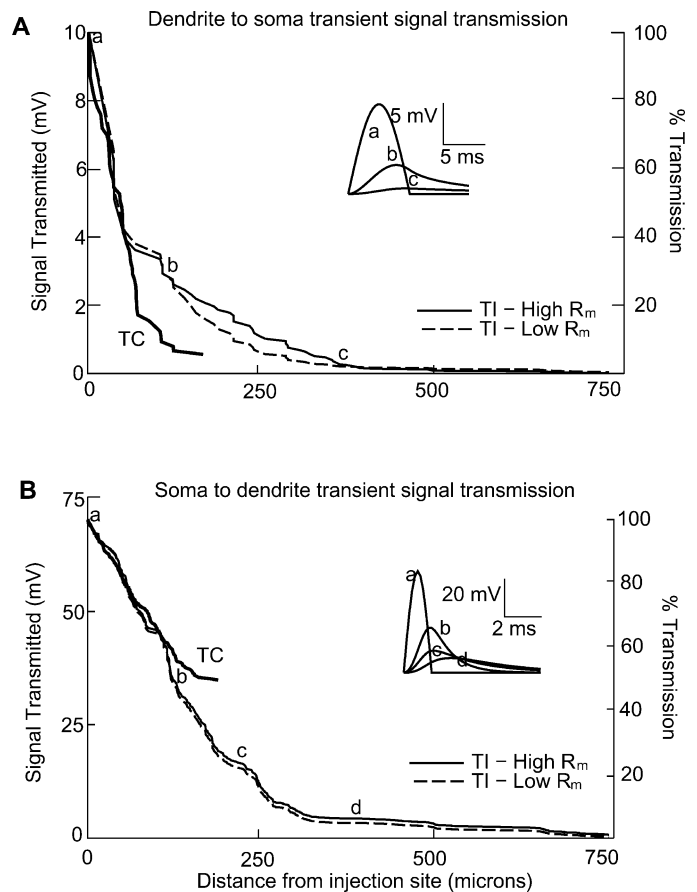

FIG. 4. Greater attenuation for transient signals: insets show representative signals at the indicated locations. (A) Orthodromic transmission of 10 mV, 5 ms signal. Voltage signal (PSP analogue) was clamped at locations throughout the dendritic tree, measured at the soma and averaged by location. Fall-off is similar for high and low R_m. Abscissa values are distances from injection site to soma. (B) Antidromic transmission of 70 mV, 2 ms signal. Voltage signal (AP analogue) was clamped at the soma and measurements were made at locations throughout the dendritic tree and averaged by location.

capacitance does not occur physiologically. We used this artifactual manipulation to demonstrate that transient signal transmission is dependent on capacitance rather than on the biologically varying membrane resistance. By preserving the high R_{in} of the interneuron, but reducing C_m 15-fold, transmission at the distal dendrites jumped from 1 to 10 mV.

We also explored the effect on single-signal propagation of a five-fold reduction in R_m (Fig. 4). In contrast to the steady-state case, R_m reduction had little effect on transient signal transmission; lowering R_m decreased the transmitted signals by <10% for both cell types with both directions.

Burst signal

Often, synaptic inputs and action potentials come not singly but in rapid trains or bursts. Burst firing is particularly characteristic of thalamic cell responses in the sleep state (Steriade *et al.*, 1990). We found that bursts of EPSP–IPSP and AP analogues were carried more readily down the dendrite than were isolated signals (Fig. 5). This was due to the fact that bursts provide both greater total current injection and increased time over which the input arrives, creating a signal
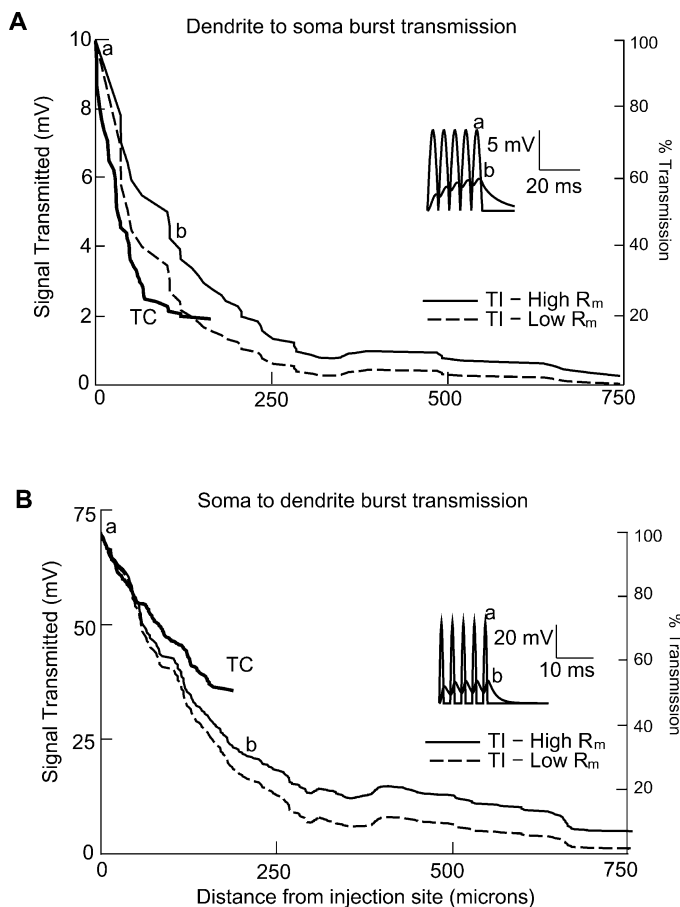

FIG. 5. Burst transmission: bursts show greater transmission than single signals. (A) Orthodromic transmission of five-signal bursts (10 mV, 5 ms). Voltage signal (PSP burst analogue) was clamped at locations throughout the dendritic tree, measured at the soma and averaged by location. High and low R_m produced different transmission values (shown for interneuron). Abscissa values are distances from injection site to soma. Inset compares (a) voltage from a location 150 μm out to (b) voltage in the soma. (B) Antidromic transmission of five-signal bursts (70 mV, 2 ms). Voltage signal (AP burst analogue) was clamped at the soma and measurements were made at locations throughout the dendritic tree and averaged. Inset compares (a) voltage in the soma to (b) voltage at a location 225 μm out.
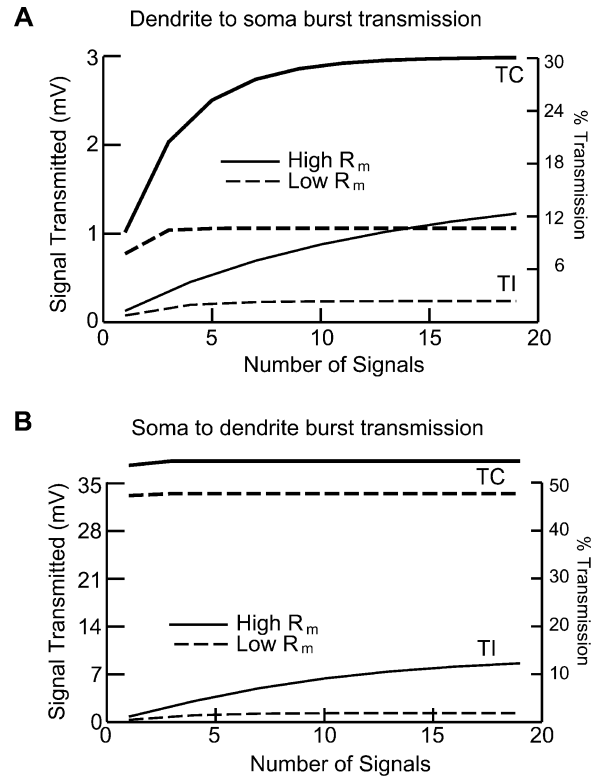

FIG. 6. Differential transmission of different-length bursts. (A) Orthodromic transmission (PSP analogue: 10 mV/5 ms). Signal was placed at several locations two-thirds of the way out in the dendrites and maximal somatic voltages were measured and averaged for different-length 200-Hz bursts. (B) Antidromic transmission: 200 Hz AP burst analogue (70 mV/2 ms) was clamped at the soma and measured at several locations two-thirds of the way out in the dendrites. Maximal voltages were measured and averaged for different-length bursts.

intermediate between single transient and steady-state signals. As found with steady-state signals, changing from high to low R_m substantially augmented signal drop-off.

We varied number of signals during a burst with spike frequency 200 Hz in order to determine transmission saturation: the point where additional transient signals do not produce any additional depolarization at the distant measurement point (Fig. 6). Orthodromically, we found a substantial difference between the high-R_m cases and low-R_m cases. Thalamocortical cells allowed a maximal transmission of 30% (3.0 mV) in the high-R_m cases and only 9% (0.8 mV) in the low-R_m cases (Fig. 6A). The thalamocortical cell could distinguish the number of signals considerably better in the high-R_m case, with soma voltage increasing to 90% of plateau with increasing number of EPSP–IPSPs up to a count of seven. In the low-R_m case, signal integration was seen for one to three EPSP–IPSPs, with no further integration occurring with more prolonged input bursts. The interneurons also showed a greater ability to differentially transmit multiple EPSP–IPSPs in the high-R_m case, saturating with a transmission of 13% (1.2 mV) only after 26 signals (Fig. 6A). The low-R_m cell saturated at 2% (0.2 mV) after five signals. Although these interneuron voltages are quite low compared to those required for action potential generation in the soma, more proximal inputs and spatial summation could produce significant integration effects.

Antidromically, we found that the thalamocortical cell bursts did not produce significant integration in either the low-R_m case or high-R_m case (Fig. 6B). Maximal signal was 53% (33.8 mV) for the high-R_m cases and 48% (28.4 mV) for the low-R_m cases, saturating after two

signals in both cases. By contrast, interneurons showed integration up to 17 signals in the high-R_m case (plateau 9.4 mV) and up to six signals in the low-R_m case (plateau 0.9 mV).

We also looked at frequency dependence of signal integration, evaluating transmission as a function of frequency for bursts of five PSPs or APs. We considered temporal integration to be occurring if the peak voltage obtained after the burst was >10% more than that of a single signal. For thalamocortical cells, high-R_m cells were able to integrate signals of >40 Hz orthodromically, and low-R_m cells were able to integrate signals of >90 Hz. Once again, the interneurons showed a greater ability to integrate burst signals. Orthodromically, the high-R_m cases integrated bursts >20 Hz in the high-R_m case and >50 Hz in the low-R_m case. Antidromic AP integration required considerably higher frequencies in the thalamocortical cell: frequencies of 150 Hz under high-R_m conditions and of 190 Hz under low R_m. In the interneuron, on the other hand, antidromic AP signal summation occurred at frequencies similar to that seen orthodromically (24 Hz for high R_m, 50 Hz for low R_m).

Passive normalization

Previous studies have emphasized the normalizing effect of the synaptic conductance change that causes most synaptic potentials (Chitwood *et al.*, 1999; Jaffe & Carnevale, 1999). They noted that high input impedance in distal dendrites permitted higher voltage transients locally that compensated for the signal decrement with transmission to the soma. They termed this passive normalization, predicting that somatic recordings of EPSPs would show little amplitude variation despite different distances of the synapses.

To look at passive normalization in thalamic neurons, we simulated a 500-pS conductance increase in an excitatory synapse ($E_{syn} = 0$ mV, duration ≈5 ms). EPSP size was larger in more distal dendrites. In the thalamocortical cell, a proximal input produced a <1 mV voltage transient, whereas the more distal inputs produced EPSPs >10 mV in height. For the interneuron, the amplification of EPSP size was even more pronounced, as proximal inputs only caused a 2-mV signal whereas the more distal inputs could produce an EPSP >30 mV in amplitude (Fig. 7A). Recording the size of the signal transmitted to the soma we found that, for the thalamocortical cells, the larger EPSPs in the distal dendrites compensated for the larger attenuation, producing passive normalization. Inputs anywhere in the tree produced similar signals in the soma (Fig. 7B, thick line).

In the interneurons, however, somatic EPSPs showed large variability in signal amplitude, with reduced amplitude with increasing distance of synapse from soma. Proximal synapses transmitted ≈2 mV to the soma. Distal dendrites transmitted ≈0.5 mV to the soma (Fig. 7B, thin line). Lowering the membrane resistance five-fold reduced signal transmission significantly (Fig. 7B, dashed line), an effect more pronounced than seen with the voltage-clamped PSP (Fig. 4A). Lack of passive normalization in interneurons was due to two factors. First, distal inputs were reduced disproportionately because the extremely long dendrites attenuated these signals greatly. Second, many proximal inputs were boosted through the high R_{in} associated with localization in terminal interneuron dendrites which ended relatively close to the soma. By contrast, the thalamocortical cell dendrites were relatively uniform.

Bursts of conductance-synapse EPSPs showed better spread down the dendrite than did single signals (Fig. 7C). The thalamocortical cell again showed fairly uniform transmission from the different locations on the dendrites, varying from 1.0 to 1.2 mV. The interneurons again showed a larger difference in transmission from the proximal and the distal dendrites, with ≈3 mV transmission from proximal dendrites and ≈1 mV from the distal dendrites (Fig. 7C, thin lines). Lowering the
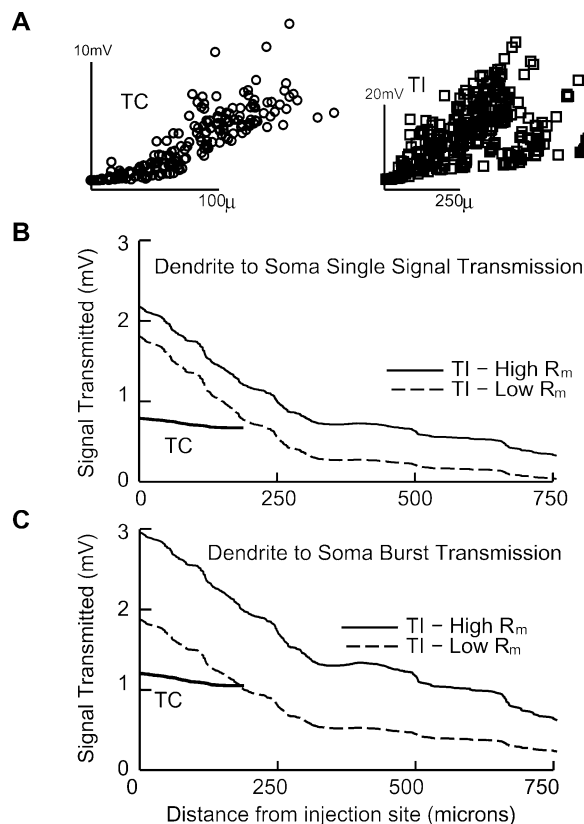

FIG. 7. Passive normalization seen in thalamocortical cells but not in interneurons (alpha function, linear rise and exponential fall: $\bar{g}$, 500 pS; E_{syn}, 0 mV; τ, 5 ms). (A) Synaptic amplification with distance. The amplitude of identical synapses is shown for every compartment in one thalamocortical cell and one interneuron. For the thalamocortical cell, scaling is roughly proportional to distance from soma; the interneuron shows considerable scatter. (B) Transient conductance change (EPSP) signal, presented in all compartments at the given distance and then measured in the soma. The thalamocortical cell shows little change with distance (passive normalization is present); the interneuron shows significant fall-off with distance (no passive normalization). (C) Burst of five EPSPs at 200 Hz presented in all compartments at the given distance and then measured in the soma. Again, the thalamocortical cell shows passive normalization and the interneuron does not. (For B and C, abscissa values are distances from injection site to soma.)

R_m in the interneuron cells decreased the signal transmission of the bursts (Fig. 7C, dashed line).

Discussion

The thalamic network is notable for the presence of a large number of dendrodendritic synapses, which suggests that signal processing in the thalamus may differ markedly from Cajal's theory of dynamic polarization: signal flow from dendrites to soma to axon. In this study, we assessed the implications of the passive properties for signal processing in the two major cell types of the lateral geniculate nucleus: thalamocortical cells and interneurons. As previously found (Bloomfield & Sherman, 1989; Neubig & Destexhe, 2001), the thalamocortical cells were electrotonically compact; the interneurons were not, due primarily to the size of their very large dendritic tree. Additionally, we confirmed the Neubig & Destexhe (2001) observation of relatively poor transmission of biologically relevant voltage transients. Electrical 'compactness' is defined by steady-state measures and does not describe transmission of postsynaptic or action potentials. Of note,

however, is that bursts could serve to alleviate this limitation on transient transmission by producing more prolonged signals. Thus, bursting could enhance signal transmission through the dendritic tree.

In this initial study, we have not included active voltage-sensitive ion channels, although such channels have been demonstrated in both thalamocortical cells and interneurons (Budde *et al*., 1998). Active channels will have a profound effect on signal transmission in dendrites. However, passive membrane parameters and cell morphology provide the baseline on which active properties act and will still be important determinants of signal transmission. Additionally, these determinants need to be defined and assessed as a preliminary to subsequent studies of active channel effects. Examination of two morphologically distinct cell types with different membrane parameters revealed a set of general, robust properties which will still be relevant even as the active channels boost, mould and manoeuvre signals through the dendrites.

In vivo, passive membrane will be locally perturbed not only by active conductances but also by local synaptic activity that will not generally be spatially uniform. Although we did not make any direct attempt to replicate this nonhomogeneity, we did assess a five-fold decrease in input resistance that would approximate to the *in vivo–in vitro* difference (Neubig & Destexhe, 2001).

Parameter definition

The *in vitro* values of R_m and C_m were well constrained from somatic recordings. For thalamocortical cells and interneurons, the two cells of the same type provided similar values for R_m in independent fits. This was not surprising, because the cells of each type were of similar size and R_{in}. Small changes in R_m provided significant changes in the input resistance of the models. Similarly, C_m was well constrained by the cell time constant. We assumed that both R_m and C_m had consistent values throughout a single cell, and we obtained these parameters from an inactive cell near its resting membrane potential. However, R_m is labile and can be modified markedly by factors such as the opening or closing of K$^+$ channels by neuromodulators such as acetylcholine. R_m will also be reduced *in vivo* by ongoing conductances associated with the synaptic bombardment of ongoing neural activity (Bernander *et al*., 1991). It has generally been assumed that C_m is a biological constant, dependent on the uniform thickness and dielectric constant of the lipid bilayer. However, recent studies have estimated C_m from 0.5 to $3 \mu Fcm^{-2}$, calling into question the constancy of this value (Chitwood *et al*., 1999). Our fitting agreed with the generally accepted value of $1 \mu Fcm^{-2}$.

In contrast to the other basic parameters, it is difficult to obtain a reliable value for axial resistance (R_a). In several cases, R_a has been shown to be unobtainable through the fitting of charging curves obtained from the usual somatic recordings (Kapur *et al*., 1997a,b; Chitwood *et al*., 1999), which suggests the need for simultaneous soma and dendrite impalement, currently impossible in cells with long, thin dendrites such as the interneurons. In this study, although we were able to get a reasonable value for R_a in the thalamocortical cells during parameter fitting, this value was not reliable because small changes in the parameters to the fitting algorithm could produce values from 50 to $200 \Omega cm$. On the other hand, we did obtain a consistent value when fitting charging curves for the interneurons (Fig. 2B and C). In the thalamocortical cells, large-calibre dendrites provided easy membrane access from the soma, regardless of specific cytoplasmic resistivity; in the interneurons, narrow, long dendrites restricted current flow which could then be augmented by reduction of R_a. In the interneurons, R_a controlled the amount of accessible membrane, producing substantial variation in the resulting values of R_{in} and τ_m. The value of $70 \Omega cm$ for R_a which we obtained from interneuron fitting is consistent with values

obtained through direct recordings from dual impalement of soma and dendrite in neocortical pyramidal cells (Stuart & Spruston, 1998). In general it should be possible to determine R_a from somatic measurements in other cell types with long, thin dendrites. Obtaining a good estimate for R_a will, however, depend on having accurate cell geometry.

Steady-state signal spread

This study was originally designed to update previous studies by utilizing physiological measurements obtained from whole-cell patch recordings rather than sharp electrode impalement. Whole-cell patch provides a much tighter seal with the neuron and therefore demonstrates higher input impedances and longer time constants which are more accurate than those obtained with sharp electrodes (Staley *et al*., 1992). Higher input impedance would be expected to arise from a higher value for membrane resistance that would in general translate to greater length constants and a more compact cell. Additionally, our explorations confirmed previous results (Neubig & Destexhe, 2001) that showed: (i) less transmission of transient than continuous signals; (ii) the need to include the full complexity of the dendritic tree rather than an abbreviated version thereof (Bloomfield & Sherman, 1989).

Transient signal spread

While steady-state signal spread was proportionately sensitive to alterations in R_m, transmission of a single pulse was only slightly modified by changes in this parameter. In contrast to the steady-state signal, which was only affected by loss of current through the resistive limb in each compartment, a brief pulse depends not only on the membrane resistance but also on the capacitance. As is known from cable theory, the effective length constant depends on signal frequency, with high-frequency spread primarily dependent on R_a and C_m and low-frequency spread dependent on R_m and C_m. For this reason, spread of our transient signal was much more sensitive to changes in C_m than to changes in R_m. Transmission of brief signals is only slightly affected by changes in R_m. This independence of R_m implies that, unlike steady-state signals, passive transmission of single spikes and PSPs is governed strongly by the geometry of the cell and is relatively independent on the neuromodulatory effects that alter the passive membrane parameters.

For single signals, the length of the interneuron dendrites produced severe attenuation and the interneuron distal dendrites may thus be expected to function as independent domains. In the thalamocortical cells, though, the much wider and shorter dendrites and the soma tend to dominate signal responses, providing for superior antidromic transmission and impaired orthodromic transmission. In order for a brief dendritic input to have substantial impact on the thalamocortical cell, it would have to coincide with the arrival of another input, a result consistent with experimental observations at the retinogeniculate synapse (Mastronarde, 1987; Usrey *et al*., 1998) and with the Neubig & Destexhe (2001) hypothesis of relatively independent thalamocortical cell dendritic clusters.

Passive normalization

Passive normalization is a term used to describe the compensation of dendritic attenuation by augmented EPSP size due to increased local input impedance in dendrites (Chitwood *et al*., 1999; Jaffe & Carnevale, 1999). As a result, EPSPs transmitted from different points in the dendritic tree are of similar size. Conductance changes generated further out in the dendrites produce larger voltages due to the higher local R_{in} associated with the thinner dendrite. This voltage boost largely compensates for the greater voltage attenuation of signals from distal dendrites in somatic recordings, leading to signal

invariance with stimulation in different dendritic locations as measured in the soma.

This effect depends on the synapse being a current injection, or a conductance change that approximates current injection, and would not be seen with our voltage-clamp PSP model. We therefore repeated our simulations using conductance synapses. Passive normalization was seen in the thalamocortical cells, but not in the interneurons. Although augmentation of the PSP in the distal dendrites was actually greater in the interneuron than in the thalamocortical cell (Fig. 7A), the long dendrites of the interneurons produced far greater signal drop-off and prevented this increase from normalizing the size of the PSP at the soma. Also, unlike the thalamocortical cells, which have dendrites of fairly uniform length and diameter, the interneuron dendrites have many short, thin, proximal branches, which showed the same amplification of PSP amplitude without the attenuation of the distant branches. Consequently, there was local amplification of the input signal at both proximal and distal dendrites and no overall normalization in interneurons. Another effect that could oppose passive normalization would be saturation of the conductance synapses. This would allow membrane potential to approach reversal potential for the synapse, leaving no room for additional signal augmentation. This was not an effect in our simulations, where the largest distal EPSPs depolarized by only $\approx$35 mV (Fig. 7A).

Thalamocortical cell dendrites are known to have active channels and it seems likely that interneuron dendrites do as well. Additionally, there is substantial postsynaptic potential amplitude variability from a variety of causes which is a dominant cause of synaptic amplitude variation (Neubig, 1999). Despite this, the differences in local input resistance noted in the passive normalization hypothesis will likely boost distal inputs.

Burst synergy

Bursts produced significantly more transmission than single signals because bursts produce a more prolonged depolarization that approaches the ongoing depolarization of a steady-state signal. This gradual transition from the single pulse to steady-state gives the cell the ability to distinguish different types of bursts, differing either by length (number of signals) or frequency. As was the case for other signal types, the interneurons showed superior orthodromic burst transmission and the thalamocortical cells showed better antidromic transmission. Both thalamocortical cell and interneuron were able to integrate multiple signals, with the interneurons showing exceptional ability to do temporal summation, integrating over 25 successive inputs.

As in the steady-state case, but unlike the single signal case, there was a considerable difference between the low-R_m case and the high-R_m case, because higher R_m provided both tighter membrane for preventing current loss and longer time constant for allowing a greater time over which inputs could be integrated (Fig. 6). A five-fold change in R_m could produce up to an eight-fold scaling in the amount of the signal transmitted.

Implications for circuitry

The thalamus shows two functional states. The awake state is dominated by segregated tonic firing relaying sensory information, whereas the sleep state tends more towards burst firing and slow widespread oscillations (Steriade *et al.*, 1990). In this study, we have shown that efficiency of passive transmission along dendrites will vary widely depending on the type of signal. Transmission of single brief signals is inefficient, with signals originating more than 100 µm from the soma being substantially attenuated. Bursts show much better transmission (Figs 4 and 6). Given the preferential transmission of bursts, the

transition to sleep may provide a functional 'shortening' of dendrites favouring the coordinated firing between neurons seen in this state.

As expected, modelling data obtained from whole-cell clamp yielded steady-state transmission showing interneurons to be more compact by this measure than previously believed. However, the more physiologically relevant transient signals were transmitted poorly, particularly in the orthodromic direction from distal dendrites to the soma. Thus, synaptic inputs to interneurons would be expected to have local influence only without integrating with presynaptic signals elsewhere in the interneuron or being transmitted via the axon to more distant cells. The distal presynaptic dendrites of interneurons would be operating independently of other dendritic branches and of the soma, the 'independent dendritic domain' scenario previously proposed for interneurons on the basis of anatomical and physiological evidence.

As a consequence of neuron morphology, antidromic signals are transmitted more effectively than orthodromic signals, given the much greater ability of soma and proximal dendrites to sink current. Assuming that interneuron action potentials are generated in soma, rather than in axon initial segment, bursts of somatic action potentials could back-propagate up the dendritic tree to affect dendrodendritic synapses, allowing axonal and dendritic outputs to act in concert. By contrast, intermediate distance synaptic inputs would propagate more easily towards distal dendrites and relatively poorly towards the soma, tending again to produce dendritic activity independent of the soma (Cox *et al.*, 1998; Cox & Sherman, 2000).

Signal spread variation would allow interneurons to contribute differentially to the thalamic circuit depending on both state and on signal type. In tonic firing mode, an individual interneuron could provide a set of input–output modules working independently of each other. This multiplexing of inhibition could provide selective sculpting of sensory information. When an interneuron produces a burst of action potentials (Zhu *et al.*, 1999b) the axonal and dendritic output could act more in unison. This effect might contribute to widespread synchrony seen during spindle oscillations. Although the contributions of interneurons to such oscillations is not clear (Krosigk *et al.*, 1993; Bal *et al.*, 1995), lesion of the spindle pacemaker, the reticular nucleus, enhanced IPSP incidence in thalamocortical cells (Steriade *et al.*, 1985) demonstrating release of interneurons from reticular GABAergic neurons and suggesting higher activities of these GABAergic local-circuit cells. In the awake state, sudden stimulus onset often results in a burst response. This would again allow the interneurons to be more functionally compact, permitting coordinated feedforward inhibitory potentials and the pronounced inhibition that is seen in thalamocortical cells in this setting.

Abbreviations

AP, action potential; C_m, membrane capacitance; EPSP, excitatory postsynaptic potential; EPSP–IPSP, EPSP–IPSP sequence; IPSP, inhibitory postsynaptic potential; λ, length constant; PSP, postsynaptic potential; R_a, axial resistance; R_{in}, input resistance; R_m, membrane resistance; τ_m, membrane time constant.

References

Bal, T., von Krosigk, M. & McCormick, D.A. (1995) Role of the ferret perigeniculate nucleus in the generation of synchronized oscillation in vitro. *J. Physiol. (Lond.)*, **483**, 665–685.

Bernander, O., Douglas, R., Martin, K. & Koch, C. (1991) Synaptic background activity influences spatiotemporal integration in single pyramidal cells. *Proc. Natl Acad. Sci. USA*, **88**, 11569–11573.

Bloomfield, S. & Sherman, S.M. (1989) Dendritic current flow in relay cells and interneurons of the cat's lateral geniculate nucleus. *Proc. Natl Acad. Sci. USA*, **86**, 3911–3914.

Briska, A., Uhlrich, D.J. & Lytton, W.W. (1999) Passive properties and signal synergy in thalamic cells. *Soc. Neurosci. Abstr.*, **25**, 8483.

Budde, T., Munsch, T. & Pape, H.-C. (1998) Distribution of L-type calcium channels in rat thalamic neurones. *Eur. J. Neurosci.*, **10**, 586–597.

Chitwood, R.A., Hubbard, A. & Jaffe, D.B. (1999) Passive electrotonic properties of rat hippocampal CA3 interneurones. *J. Physiol. (Lond.)*, **515**, 743–756.

Cox, C.L. & Sherman, S.M. (2000) Control of dendritic outputs of inhibitory interneurons in the lateral geniculate nucleus. *Neuron*, **27**, 597–610.

Cox, C.L., Zhou, Q. & Sherman, S.M. (1998) Glutamate locally activates dendritic outputs of thalamic interneurons. *Nature*, **394**, 478–482.

Hamos, J.E., Van Horn, S.C., Raczkowski, D., Uhlrich, D.J. & Sherman, S.M. (1985) Synaptic connectivity of a local circuit neurone in lateral geniculate nucleus of the cat. *Nature*, **317**, 618–621.

Hines, M. (1993) NEURON – a program for simulation of nerve equations. In Eeckman, F. (ed.), *Neural Systems: Analysis and Modeling.* Kluwer, Norwell, MA, pp. 127–136.

Hines, M. (1994) The NEURON simulation program. Skrzypek, J. (ed.), *Neural Network Simulation Environments.* Kluwer, Norwell, MA, pp. 147–163.

Jaffe, D.B. & Carnevale, N.T. (1999) Passive normalization of synaptic integration influenced by dendritic architecture. *J. Neurophysiol.*, **82**, 3268–3285.

Jones, E.G. (1985) *The Thalamus.* Plenum Press, New York.

Kapur, A., Pearce, R., Lytton, W.W. & Haberly, L. (1997a) GABAA-inediated IPSCs in piriform cortex have fast and slow components with different properties and locations on pyramidal cells: Study with physiological and modeling methods. *J. Neurophysiol.*, **78**, 2531–2545.

Kapur, A., Lytton, W.W., Ketchum, K. & Haberly, L. (1997b) Regulation of the NMDA component of EPSPs by different components of postsynaptic GABAergic inhibition: a computer simulation analysis in piriform cortex. *J. Neurophysiol.*, **78**, 2546–2559.

von Krosigk, M., Bal, T. & McCormick, D.A. (1993) Cellular mechanisms of a synchronized oscillation in the thalamus. *Science*, **261**, 361–364.

Major, G., Evans, J.D. & Jack, J.J.B. (1993a) Solutions for transients in arbitrarily branching cables. I Voltage recording with a somatic shunt. *Biophys. J.*, **65**, 423–449.

Major, G., Evans, J.D. & Jack, J.J.B. (1993b) Solutions for transients in arbitrarily branching cables. II Voltage clamp theory. *Biophys. J.*, **65**, 450–468.

Mastronarde, D.N. (1987) Two classes of single-input X-cells in cat lateral geniculate nucleus. I Receptive-field properties and classification of cells. *J. Neurophysiol.*, **57**, 357–380.

Neubig, M. (1999) Variation in GABA mini amplitude in thalamocortical neurons: contrasting experimental data and computational analyses. Ph.D. thesis, Laval University, Quebec City.

Neubig, M. & Destexhe, A. (2001) Dendritic organization in thalamocortical neurons and state-dependent functions of inhibitory synaptic inputs. *Thalamus and Related Systems*, **1**, 39–52.

Pasik, P., Pasik, T. & Hamori, J. (1976) Synapses between interneurons in the lateral geniculate nucleus of monkeys. *Exp. Brain Res.*, **25**, 1–13.

Sherman, S.M. & Guillery, R.W. (1996) Functional organization of thalamocortical relays. *J. Neurophysiol.*, **76**, 1367–1395.

Staley, K.J., Otis, T.S. & Mody, I. (1992) Membrane properties of dentate gyrus granule cells – comparison of sharp microelectrode and whole-cell recordings. *J. Neurophysiol.*, **67**, 1346–1358.

Steriade, M., Deschênes, M., Domich, L. & Mulle, C. (1985) Abolition of spindle oscillations in thalamic neurons disconnected from nucleus reticularis thalami. *J. Neurophysiol.*, **54**, 1473–1497.

Steriade, M., Jones, E.G. & Llinas, R.R. (1990) *Thalamic Oscillations and Signaling.* Wiley, New York.

Storm, J.F. (1990) Why is the input conductance of hippocampal neurones impaled with microelectrodes so much higher than when giga-seal patch pipettes are used? *Soc. Neurosci. Abstr.*, **16**, 506.

Stuart, G. & Spruston, N. (1998) Determinants of voltage attenuation in neocortical pyramidal neuron dendrites. *J. Neurosci.*, **18**, 3501–3510.

Usrey, W.M., Reppas, J.B. & Reid, R.C. (1998) Paired-spike interactions and synaptic efficacy of retinal inputs to the thalamus. *Nature*, **395**, 384–387.

Wathey, J., Lytton, W.W., Jester, J. & Sejnowski, T. (1992) Computer simulations of EPSP–spike (E–S) potentiation in hippocampal CAI pyramidal cells. *J. Neurosci.*, **12**, 607–618.

Wilson, J.R., Friedlander, M.J. & Sherman, S.M. (1984) Fine structural morphology of identified X- and Y-cells in the cat's lateral geniculate nucleus. *Proc. Roy. Soc. Lond. .B. Biol. Sci.*, **221**, 411–436.

Zhu, J.J., Lytton, W.W., Xue, J.T. & Uhlrich, D.J. (1999c) An intrinsic oscillation in interneurons of the rat lateral geniculate nucleus. *J. Neurophysiol.*, **81**, 702–711.

Zhu, J.J., Uhlrich, D.J. & Lytton, W.W. (1999a) Properties of a hyperpolarization-activated cation current in interneurons in the rat lateral geniculate nucleus. *Neuroscience*, **92**, 445–457.

Zhu, J.J., Uhlrich, D.J. & Lytton, W.W. (1999b) Burst firing in identified interneurons of the rat lateral geniculate nucleus. *Neuroscience*, **91**, 1445–1460.